ISTANBUL TECHNICAL UNIVERSITY ★ GRADUATE SCHOOL

DEVELOPMENT OF MULTI-CAPSULE ENDOSCOPY LOCOMOTION VIA SPRING ASSISTED DISTANCE MANAGEMENT

M.Sc. THESIS

Erfan PARSAEI

Department of Electronics and Communication Engineering

Biomedical Engineering Program

JUNE 2025

ISTANBUL TECHNICAL UNIVERSITY ★ GRADUATE SCHOOL

DEVELOPMENT OF MULTI-CAPSULE ENDOSCOPY LOCOMOTION VIA SPRING ASSISTED DISTANCE MANAGEMENT

M.Sc. THESIS

Erfan PARSAEI
(504221402)

Department of Electronics and Communication Engineering

Biomedical Engineering Program

Thesis Advisor: Prof. Dr. Onur FERHANOĞLU

JUNE 2025

ISTANBUL TEKNİK ÜNİVERSİTESİ ★ LİSANSÜSTÜ EĞİTİM ENSTİTÜSÜ

YAY DESTEKLİ MESAFE KONTROLÜ İLE ÇOKLU KAPSÜL ENDOSKOPİ LOKOMOSYONUNUN GELİŞTİRİLMESİ

YÜKSEK LİSANS TEZİ

Erfan PARSAEI
(504221402)

Elektronik ve Haberleşme Mühendisliği Bölümü

Biyomedikal Mühendisliği Programı

Tez Danışmanı: Prof. Dr. Onur FERHANOĞLU

HAZİRAN 2025

Erfan PARSAEI, a M.Sc. student of İTU Graduate School student ID 504221402, successfully defended the thesis entitled “DEVELOPMENT OF MULTI-CAPSULE ENDOSCOPY LOCOMOTION VIA SPRING ASSISTED DISTANCE MANAGEMENT”, which he prepared after fulfilling the requirements specified in the associated legislations, before the jury whose signatures are below.

Thesis Advisor : **Prof. Dr. Onur FERHANOĞLU** ....
Istanbul Technical University

Jury Members : **Assoc. Prof. Dr. Ali Fuat Ergenç** ....
Istanbul Technical University

Assoc. Prof. Dr. Yiğit Dağhan Gökdel ....
Istanbul Bilgi University

Date of Submission : 27 May 2025
Date of Defense : 17 June 2025

To my spouse and parents,

FOREWORD

Finishing this thesis has been a hard but very gratifying journey, and I want to thank everyone who has helped me along the way. At the top is my respected advisor, Professor Dr. Onur Ferhanoğlu, whose advice, wisdom, and constant support have been very helpful in making this work. I also want to thank Furkan Peker for their helpful comments and support. I also want to thank my family and friends for always being there for me and supporting me during this difficult but rewarding project.

June 2025

Erfan PARSAEI
(Biomedical Engineering)

TABLE OF CONTENTS

Page

ABBREVIATIONS

CAD	Computer-Aided Design
CMOS	Complementary Metal-Oxide Semiconductor
COMSOL	COMSOL Multiphysics
DC Motor	Direct Current Motor
DOF	Degree of Freedom
EMA	Electromagnetic Actuation
EPM	Electromagnetic Platform or Permanent Magnet (context-specific)
FEM	Finite Element Method
GI	Gastrointestinal
MASCE	Magnetically Actuated Soft Capsule Endoscope
MFN	Magnetic Field Navigator
PC	Personal Computer
PLA	Polylactic Acid
ROC	Radius of Curvature
SCARA	Selective Compliance Assembly Robot Arm
SMA	Shape Memory Alloy
WCE	Wireless Capsule Endoscopy

SYMBOLS

R	: Minimum radius of curvature of the GI tract
R_c	: Radius of the capsule
L	: Maximum allowable extended spring length
F_k	: Force in the spring
F_1, F_2	: Forces acting on capsule 1 and capsule 2
x_1, x_2	: Displacement of capsule 1 and capsule 2
$\dot{x_1}$, $\dot{x_2}$	: Velocity of capsule 1 and capsule 2
$\ddot{x}_2$, $\ddot{x}_1$	: Acceleration of capsule 1 and capsule 2
k_{eff}	: Effective spring constant
$F_{peristalsis}$	: Peristaltic force acting on the capsule
n	: Number of coils in the spring
d	: Average coil diameter of the spring
$\delta(t)$	: Dirac delta function (for instantaneous perturbations)
d_c	: Capsule diameter
l_c	: Capsule length
l_s	: Spring length
d_s	: Spring diameter
g	: Spring gap
d_h	: Magnet holder diameter
l_h	: Magnet holder length
E	: PLA Young’s modulus
ρ_{pla}	: PLA density
ν	: Poisson’s ratio
k	: Spring constant
m	: Mass (of capsule)

LIST OF TABLES

Page

LIST OF FIGURES

Page

DEVELOPMENT OF MULTI-CAPSULE ENDOSCOPY LOCOMOTION VIA SPRING-ASSISTED DISTANCE MANAGEMENT

SUMMARY

Gastrointestinal (GI) tract analysis has been revolutionized since the emergence of wireless capsule endoscopy (WCE) in 2000 and has been widely accepted due to its minimally invasive procedures. While conventional GI examinations, such as colonoscopy and endoscopy, involve sedation and multiple insertions, capsule endoscopy offers a more compliant alternative for analyzing the GI tract for patients.

Traditional WCE systems were mainly focused on imaging, which limited their usability in advanced medical procedures like biopsy, drug delivery, and real-time diagnostics. To overcome such drawbacks, the concept of a multi-WCE train was introduced, where instead of one, multiple capsules synchronously operate to enhance diagnostic and therapeutic capabilities.

Ensuring the stable connection of the multi-capsule endoscopy was a primary challenge in WCE train procedures, particularly in sharp turns of the intestinal paths. Previous studies have worked on coil-based inductive power systems and magnetic-based remote actuation to support the intercapsule connection. However, these methods have faced drawbacks during complex GI tract paths. This study aims to overcome these challenges by introducing a new capsule configuration with flexible spiral springs and embedded spherical magnets. This system supports a stable connection between capsules during sharp radius of curvatures (ROCs) of the intestinal path.

We proposed a system that consists of multiple capsules, each designed with a special spiral spring equipped with a permanent magnet. These springs allow the capsule train to connect firmly during the entire examination, especially in sharp turns of the bowel paths. This approach provides a physical yet adaptable connection mechanism that does not rely on external power sources. The spring's flexible characteristics adapt to the changes in the inter-capsule distance during movement, ensuring the train remains intact during harsh paths.

The evaluation of the effectiveness of this approach was conducted by using finite element analysis, beside physical experiments. The COMSOL multiphysics simulations were focused on assessing the mechanical properties of the model, including K-value evaluations of the springs, yield point, stress distribution under the known forces, and displacement of the spiral springs.

Three different intestinal models were used to conduct physical experiments to test various capsule-spring configurations: a basic polylactic acid (PLA) phantom, a silicone-coated bowel model with villus-like shape, and a bovine bowel-covered intestinal model for mimicking the realistic scenarios.

YAY DESTEKLİ MESAFE KONTROLÜ İLE ÇOKLU KAPAÜLÜ ENDOSKOPİ LOKOMOSYONUNUN GELİŞTİRİLMESİ

ÖZET

Geleneksel endoskopik yöntemler, gastrointestinal (GI) sistemin incelenmesinde önemli rol oynamaktadır. Ancak bu yöntemler sedasyon gerektirmesi, sınırlı ulaşılabilirlik ve hasta konforunu olumsuz etkilemesi gibi nedenlerle zaman içinde yerini daha az invaziv tekniklere bırakmaya başlamıştır. Bu bağlamda kablosuz kapsül endoskopisi (wireless capsule endoscopy, WCE), özellikle ince bağırsağın incelenmesinde önemli avantajlar sunarak modern tanı araçları arasında yerini almıştır. Yine de, WCE sistemleri hareket kabiliyeti ve yönlendirme açısından önemli sınırlamalara sahiptir. Özellikle pasif kapsül yapısı nedeniyle kapsülün belirli bir bölgede sabitlenememesi, yön kontrolünün olmaması ve kıvrımlı bağırsak bölgelerinde ilerleyememesi, bu sistemin işlevselliğini kısıtlamaktadır.

Bu tez çalışması, bu sınırlamaları aşmak amacıyla, yay destekli mesafe kontrolü ile çalışan ve birbirine fiziksel olarak bağlanmış çoklu kapsülden oluşan bir kapsül treni geliştirmeyi hedeflemektedir. Sistem, kapsüller arasındaki bağlantının spiral yaylar ve kalıcı mıknatıslar aracılığıyla sağlandığı pasif bir mekanizmaya dayanmaktadır. Böylece kapsüller, birbirleriyle esnek ama sağlam bir şekilde bağlanarak senkronize bir hareket yapısı kazanmaktadır. Bu yapı, GI kanalında özellikle keskin dönüşlerin olduğu bölgelerde bile yapının dağılmadan ilerleyebilmesini sağlar.

Literatürde yer alan çok sayıda çalışmada kablosuz kapsül endoskopi sistemlerinin hareket kabiliyetinin artırılmasına yönelik çeşitli içten ve dıştan yönlendirme teknikleri geliştirilmiştir. İçten hareket çözümleri arasında "inchworm" benzeri yapılar, bacaklı mikromekanizmalar, titreşimle hareket eden sistemler ve vidalı ya da yüzme prensipli robotik çözümler bulunmaktadır. Bu sistemler genellikle yüksek enerji tüketimi, doku hasarı riski ve komplekslik nedeniyle klinik uygulamalarda yaygınlaşamamıştır. Öte yandan dış yönlendirme sistemleri (robotik kol, el tipi mıknatıslar, elektromanyetik alanlar vb.) daha kontrollü hareket imkânı sunsa da, genellikle pahalı, hantal ve hasta hareketini kısıtlayan yapılar sergilemektedir.

Bununla birlikte, çoklu kapsül sistemleri üzerine yapılan araştırmalar genellikle ya aktif (manyetik-coil tabanlı) kontrollere dayanmakta ya da yalnızca teorik düzeyde kalmaktadır. Literatürde İstanbul Teknik Üniversitesi bünyesinde yapılan çalışmalar, hem pasif mıknatıs yerleşimiyle hem de aktif hall sensör ve bobin sistemleriyle kapsül treni oluşturmaya çalışmıştır. Ancak bu sistemlerin keskin dönüşlerde istikrarlı bağlantıyı sağlayamaması, bu tezin yay destekli yeni yaklaşımını ön plana çıkarmaktadır.

Bu çalışmada geliştirilen sistem, her biri spiral yay ve mıknatısla donatılmış en az iki kapsülden oluşmaktadır. Kapsüller arası bağlantı, kapsül kubbelerine entegre edilen spiral yayların mıknatıslarla birbirini çekmesi sayesinde gerçekleşmektedir. Yaylar, kapsüller arası mesafeyi sabit tutmakla kalmaz, aynı zamanda GI kanalındaki peristaltik hareket sırasında esneyip büzülerek kapsül treni bütünlüğünü korur.

Sistemin tasarımı aşamasında ilk olarak maksimum yay uzama miktarı hesaplanmıştır. GI kanalındaki en dar kıvrım yarıçapı (radius of curvature, ROC) 25 mm olarak kabul edilmiş ve kapsül çapı da dikkate alınarak maksimum yay uzunluğu 18 mm olarak belirlenmiştir. Bu sınır, hem güvenlik hem de mekanik dayanıklılık açısından önemli bir tasarım kriteri olmuştur.

Ardından yay tasarımı için SOLIDWORKS ortamında farklı geometri ve sarım sayılarına sahip spiral yay modelleri oluşturulmuş; minimum yazdırma kalınlığı, kapsül kubbe çapı ve montaj kolaylığı gibi üretim parametreleri göz önüne alınmıştır. Yaylar, polilaktik asit (PLA) kullanılarak 3D yazıcıda üretilmiş ve uçlarına silindirik neodim mıknatıslar yerleştirilmiştir.

Yayların mekanik özelliklerini test etmek amacıyla COMSOL Multiphysics yazılımı ile sonlu elemanlar analizleri gerçekleştirilmiştir. Bu analizlerde PLA'nın elastik modülü, yoğunluğu ve Poisson oranı dikkate alınmış; yayların çeşitli kuvvetler altında deformasyon, gerilme dağılımı ve yay sabiti hesaplanmıştır. Analitik hesaplamalar ile finite element method (FEM) sonuçları yüksek oranda tutarlılık göstermiştir (yaklaşık 45–50.9 N/m). Bu sonuçlar, yayların hem elastik davranışlarını hem de uzun vadeli dayanıklılığını ortaya koymuştur.

Fiziksel testler için üç farklı yay konfigürasyonu (kısa, orta ve uzun) hazırlanmış; her biri farklı sarım sayısı ve uzunluklara sahiptir. Bu yaylar yine PLA'dan üretilmiş kapsüllerle birleştirilmiş ve deneysel düzeneklerde test edilmiştir.

Sistemin performansını değerlendirmek için üç ayrı GI kanal fantomu kullanılmıştır: PLA'dan üretilmiş pürüzsüz kanal, silikon kaplamalı ve villus benzeri yapılar içeren kanal, gerçek sığır bağırsağıyla kaplanmış kanal.

Her deneyde ön kapsül sabit hızda bir motor yardımıyla çekilmiş, arka kapsül yayla bağlandığı için pasif olarak sürüklenmiştir. Kapsüller üzerine yerleştirilen renkli işaretleyiciler complementary metal-oxide Semiconductor (CMOS) kamera ile takip edilmiş; hareket analizleri MATLAB ve OpenCV yazılımlarıyla yapılmıştır. Ortalama kapsüller arası mesafe, yay sertliğine göre 24.5–25.0 mm arasında değişmiştir. Bu da sistemin farklı yay konfigürasyonlarıyla dahi stabil çalışabildiğini ve GI kanalındaki kıvrımlarda bağlantının bozulmadığını göstermektedir.

Elde edilen sonuçlar, geliştirilen yay destekli bağlantı mekanizmasının hem enerji verimliliği açısından hem de güvenli hareket kabiliyeti bakımından önceki yaklaşımlardan üstün olduğunu göstermektedir. Özellikle kıvrım yarıçapı (ROC) = 25 mm gibi keskin dönüşlerde bile kapsüllerin bağlantısının korunabilmesi, literatürdeki pasif mıknatıs ya da aktif bobin sistemlerinin başaramadığı bir noktayı aşmaktadır.

Sistemin pasif çalışması sayesinde harici enerji ihtiyacı ortadan kalkarken, aynı zamanda üretim maliyetleri de düşmektedir. Yay sabitinin ayarlanabilir olması, sistemin farklı yaş gruplarına veya anatomik yapılara göre kişiselleştirilebilmesini mümkün kılar. Ayrıca yay yapısının esnekliği, peristaltik dalgalara uyum sağlayarak kapsül hareketini destekler.

Bununla birlikte, motorla çekilen deneysel düzeneklerin gerçek peristaltik kuvvetleri birebir yansıtamaması, sistemin biyolojik ortamlardaki davranışını sınırlı ölçüde gösterebilmektedir. Ayrıca açık yay yapısının biyolojik sıvılara ve dokulara uzun süreli maruziyette kapsül iç bileşenlerini etkileyebileceği düşünülerek, ileride biouyumlu koruyucu kılıfların entegre edilmesi önerilmektedir.

Sonuç olarak bu tez çalışmasında geliştirilen yay destekli çoklu kapsül tren sistemi, kapsül endoskopide çığır açabilecek yenilikçi bir yaklaşım sunmaktadır. Enerji gereksinimi olmadan çalışan bu sistem, keskin bağırsak kıvrımlarında dahi stabil bağlantı sağlar ve yönlendirme, görüntüleme sürekliliği gibi açılardan önemli avantajlar sunar. Literatürdeki diğer yöntemlere göre daha düşük maliyetli, daha güvenli ve klinik entegrasyonu kolay bir çözüm potansiyeli taşımaktadır.

Gelecekteki çalışmalar, bu sistemin üzerine aktif yönlendirme sistemlerinin entegre edilmesi, biyouyumlu kaplamaların eklenmesi ve gerçek peristaltik hareketlerle test edilmesi gibi yönlerde ilerleyebilir. Ayrıca sistemin tanı amaçlı olduğu kadar ilaç salınımı, biyopsi gibi tedavi edici özelliklerle desteklenmesi, çok işlevli kapsül tren sistemlerinin geliştirilmesine zemin hazırlayacaktır.

1. INTRODUCTION

Human GI tract abnormalities which may involve the oral cavity, pharynx, esophagus, stomach, small and large intestine, rectum, and anus, have been a frequent and essential diseases that affects millions of people anually with different severity degrees. A Wide range of conditions are included as common disorders such as inflammatory bowel disease, colon/bowel/rectal cancer, obscure GI bleeding (OGIB), and tumors appearing in the small bowel. These diseases often appear with non-specific symptoms such as pain in the abdominal area, anemia, bleeding, and unexpected weight loss that require detailed and targeted diagnostic assessments. One of the parts of the GI tract that challenges clinicians during examination procedures is the small intestine’s lengthwise nature and twisted structure, which are hard to reach with conventional endoscopic tools. Traditionally, these abnormalities were diagnosed with procedures involving tube insertion and sedation, and were limited in reach, such as colonoscopy and endoscopy. These methods were discomforting for the patients and could lead to further complications due to reactions to sedation and tube insertion, as well as delayed or missed diagnoses. In addition, in such procedures, as stated before, small intestine monitoring is more difficult as the length of the small intestine is too long for tubes to reach.

A better solution for GI tract procedures is the use of WCEs, as they are painless, can be performed without sedation and Anesthesia, and do not have limitations in reaching certain parts of the digestive system.

The development of WCE began in the 1990s when pill-shaped devices with a complementary metal-oxide semiconductor (CMOS) camera were used to monitor the GI tract, especially the small bowel. The process begins with swallowing a pill-sized capsule containing a camera, light, transmitter, etc.; after hours, the capsule travels the entire human digestive tract and is excreted naturally. After that, a gastroenterologist examines the capsule and analyzes its information, such as tumors, bleeding, inflammation, and ulcers. The PillCam SB was the first commercially available WCE system, which was used in human trials in the 2000s. Details are given in Figure 1.1.

In comparison to traditional endoscopic and colonoscopic procedures, WCE has the ability to reach and examine the inner parts of the gastro intestinal paths, like the small intestine, that leads to a more reliable diagnosis for various human digestive system problems such as inflammatory bowel disease, colon/bowel/rectal cancer, OGIB, tumors, etc.

WCE in the early stages was mainly used for imaging and monitoring applications by the use of multiple CMOS cameras. This imaging procedure was conducted and interpreted by clinicians for the early diagnosis of GI tract abnormalities. A receiver next to the patient's body gets the pictures and information that were taken during the WCE procedures. Multiple antennas send this information over a radio frequency link [3-5].

Nowadays, WCE is widely accepted and used by clinicians for numerous applications such as examinations of GI tract diseases, GI motility monitoring like pH, temperature, and pressure of the gut, drug delivery, biopsy, gas sensing, etc.

Besides this, additional capabilities were introduced through literature to enhance capsules' diagnostic accuracy and add novel treatment capabilities. Also, navigation and locomotion methods were studied through the literature for more advanced applications. The following sections will provide more information about the studies.

a) b) c)

Figure 1.1 : (a) The PillCam, developed by Given Imaging, was the first commercially available wireless capsule endoscopy that was used for GI visualization. (b) An image from an endoscopic procedure with NSAID-induced ulcers in a middle-aged female suffering from GI bleeding. (c) Image showcasing the capsule endoscopy in the large intestine [2].

1.1 Literature Review

Besides the widespread use of capsule endoscopy by clinicians, its application has been limited to imaging in commercial settings. Multiple limitations due to conventional design problems reduced the device's functionality. One study that focused on the passiveness of the capsules discussed the issues with passive WCE, which cannot stop at a desired position and might lead to capsule retention, where the examination of the GI tract might take several days [6]. Parallelly, different functionalities have been studied through the literature to introduce new techniques focusing on locomotion and navigation systems [5]: locomotion of the capsules can be addressed by two different approaches, internal and external solutions. Internal solutions could be addressed by adding an inchworm-like mechanism that moves the capsules inside the GI tract, as discussed in [9,10]. In this study, a shape memory alloy (SMA) actuator is developed, allowing the capsule configuration to stretch and contract. Also, the Inverse motion problem has been addressed by the use of a suction cup that attaches the capsule to the surface of the GI tract. Another study that also focused on two inchworm-like capsules [10, 11] in which an SMA spring with a piezoactuator is used to attain motion, besides the capsule, is equipped with microneedles to help the capsules attach to the GI tract. Slow movement speed and high power consumption are the two drawbacks of this study. Furthermore, in [12-15], another inchworm-like capsule setups were developed with SMA wires. Heat scattering may occur due to the SMA actuation nature, which can cause tissue damage in capsule-tissue contacts [15]. The length of the spring may also be a limitation for this setup, as the force generated by the actuator is proportional to its length.

Paddle/leg-based systems are another approach for internal locomotion solutions in which a couple of paddles or leg-like mechanisms are developed onto the capsules that are actuated by an inner mechanism. In this system, the navigation of the WCE setup is conducted by the actuation of these legs that move capsules forward as suggested in [16, 17]. Another study that also focuses on the paddle-based movement is indicated in [18], in which a linear movement of the WCE is mimicked by using a DC motor and a lead screw that pushes the paddles backwards to get extra movement towards the GI tract. The system repeats this process every time the direct current (DC) motor reverses. Furthermore, a study in [19] was conducted working on a 12-legged WCE supplied with two DC motors, each controlling half of the legs. In [20], the WCE is also made to move like the mucus-cilia system, which is powered by an SMA actuator. The movement speed improved in this study in comparison to the inchworm-like movement; however, the power consumption issue remains the same [21]. The backward movement in such WCE designs is not possible due to the paddles' and legs' characteristics, and also, tissue damage is a high possibility.

The crawler mobility system discussed in [22-24], the final friction-force-based mechanism, allows the capsules to mimic a car or tank movement. In these studies, a worm set is driven by a DC motor that is connected to a planetary gearbox. The WCE is moved by the protruding worm gears, which function as wheels. Via using this method, they have reached a faster capsule movement through the GI tract in comparison with earlier approaches (inchworm-like and padded/legged systems). However, disability to move backwards and the failure to anchor the capsule are two disadvantages in using such WCE.

Figure 1.2 is an indication of multiple friction-based movement methods discussed earlier.

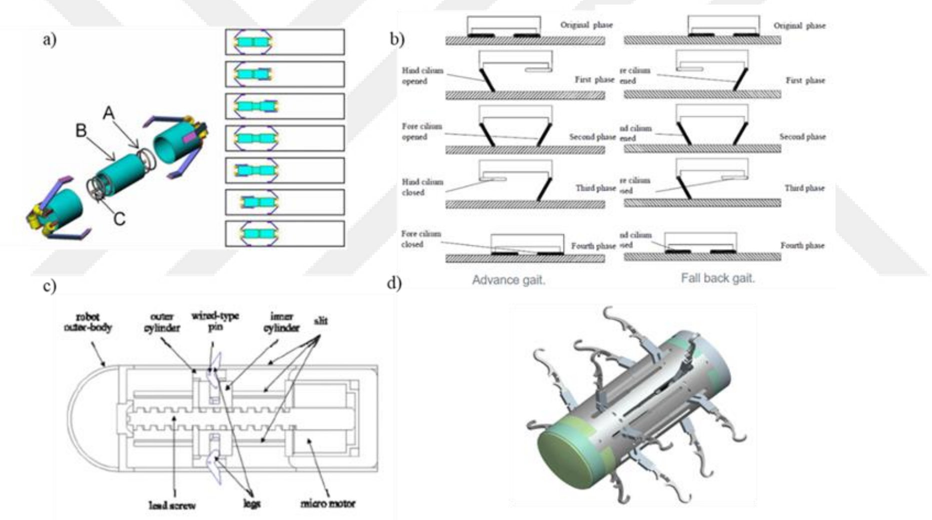

Figure 1.2: A Couple of internal-based locomotion systems discussed in literature; (a) inchworm-like [25], (b) ciliated [20], (c) legged-based [18], (d) legged [19].

An alternative approach for internal movement solution studied through the literature is the use of the swimming robots, which lean on hydrodynamic forces. This study [26] focused on the endoscopic robot that is actively actuated by a micro-motor to provide steering and straight movements. In essence, the spiral exterior structure is used to generate propulsive force without coming into contact with the intestinal wall. The steering head, which is powered by the DC motor, is made to regulate the motion in a way that accommodates the bent intestines and has the ability to move in the backward position.

Another study [27], suggested an active capsule robot that uses a screw impeller for propulsion and is intended for use in tubular, compliant settings such as the GI tract. The robot benefits from two mechanisms to move: (1) direct contact with food residue and intestinal folds, and (2) hydrodynamic fluid pressure from a fluid layer. Furthermore, a WCE with active hydrodynamic force locomotion modeling is presented in [28, 29], which is powered by four radio-controlled motors that achieve higher speeds in any direction by optimizing power. These are more power-efficient; however, the rotation capability of these systems may harm the intestinal tissue, and also lack the anchoring mechanism for advanced applications.

A vibration-based movement system is the last approach for internal locomotion solutions discussed in the studies. This study [30] overcomes the significant drawback of weak embedded batteries by transmitting >300 mW to the capsule using a 3D inductive powering module. Focuses on the incorporation of a vibratory motor for propulsion as well, using vibrations to move through tissue and fluid conditions. Although being easy to assemble and having a simple technique of locomotion is an advantage of the system, the inability to anchor the capsule to the tract and instability are the main drawbacks of this approach.

The three internal models discussed above are illustrated in Figure 1.3.

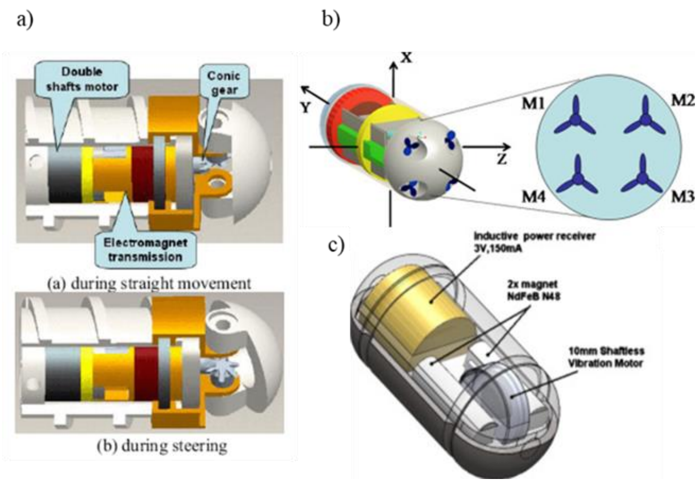

Figure 1.3: a) Swimming robots based on active WCE [26], b) WCE with a combination of hydrodynamic and friction-based locomotion, c) WCE developed with a vibratory locomotion mechanism.

The second method studied through the literature for WCE locomotion is based on external solutions to navigate capsule movement, which reduces the power usage and unstable movements discussed in the internal methods. The external methods can be categorized into 4 mechanisms:

- M1: Robotic arms equipped with magnets
- M2: handheld units developed with a permanent magnet
- M3: Subject encompassed by closed bore coil arrays
- M4: Open bore coil arrays configured above and/or below the subject

WCE developed with robotic arms (M1) have relatively better control, and due to their broad degree of freedom (DOF), which enhances their accuracy and precision. However, such WCE may harm the tissue. In one of the studies [31], a compact navigation system based on magnets (C-Mag) is utilized, which contains two electromagnets equipped to a Compliance Assembly Robot Arm (SCARA) generating a magnetic field. This robotic arm facilitates the manipulation of the WCE in a large 3D space by rotating the electromagnets. Also, this study [32] developed a magnetic-controlled capsule endoscopy that enhances the WCE functionality and mobility by introducing a robotic arm-assisted closed-loop active control of the WCE by integrating an image-based navigation system. The locomotion of the capsule endoscope is provided by a rotating magnetic field, and a gyroscope is used inside the capsule to obtain the WCE posture in the GI tract. Although this navigation and locomotion system is feasible, it is limited due to control distance because of the size of the EPM/magnetism and wiring interference from essential cables.

Capsule locomotion based on handheld units (M2) is easy to use by hand motion and reduces costs. However, this CE setup is limited in controlling the Capsule in deeper GI tract areas. One study [33] discussed the use of a hand-held magnetic field navigator (MFNs) for capsule locomotion, which involves the use of an MFN system as well as a side-magnetized CE. In the proposed system, clinicians navigate WCE motions through natural hand motions and can reach the desired viewing angle for analysis. In another study [34], they used a microcam navigation system, which involves using a handheld external magnet on the capsule and a sensor belt. This study mainly focuses on the upper GI tract, such as the cardia, fundus, and antrum.

Closed-bore control systems (M3), consisting of numerous coils, are generally configured as imaging units with a bore, such as computed tomography devices or magnetic resonance imagers, providing a greater level of freedom (5,6 DOF) at the cost of elevated expenses and increased system complexity. In [35], they developed a system that tracks the capsule inside the body using magnetic fields, which is simply achieved by placing small magnets inside the CE that create a magnetic field around the body. A set of sensors tracks the magnetic field and locates the capsule's location inside the body. The main drawback of this approach is that the movement of the patient will disrupt the magnetic field and disable the tracking of the WCE. Another study [36] focuses on a powerful electromagnetic actuation (EMA) by using eight stationary electromagnetic coils generating a powerful and flexible magnetic field. Magnetically actuated capsule endoscope (MACE) contains a permanent magnet, has five degrees of freedom, and can travel in all directions.

Finally, the last external method is a control hardware open-bore coil/electromagnetic-based control system (m4), positioned between manually operated handheld units (m1) and closed-bore arrays (m3) that utilize numerous external coils (>8) regarding design complications and affordability. It offers a more patient-friendly examination compared to closed-bore control mechanisms with multiple coils, particularly for patients suffering from claustrophobia. A study [37] suggests using magnetic energy from outside the body, which removes the battery reliance in WCE. The magnetic field controls the capsule's movement from outside the body by a magnetic drive unit that enables three degrees of freedom. The biggest disadvantage of the proposed system is that the patient should remain stationary for eight hours, which is not desirable for medical processes. Also, the study [38] suggests another motion control system by producing a dynamic electromagnetic field that is generated by two stationary sets of parallel and identical electromagnets that are placed underneath and above the targeted area. However, the presented method was limited in generating a desirable electromagnetic field consistently due to the heating of the platform, which may limit the magnets for electromagnetic field generation. Figure 1.4 illustrates the externally based locomotion methods discussed.

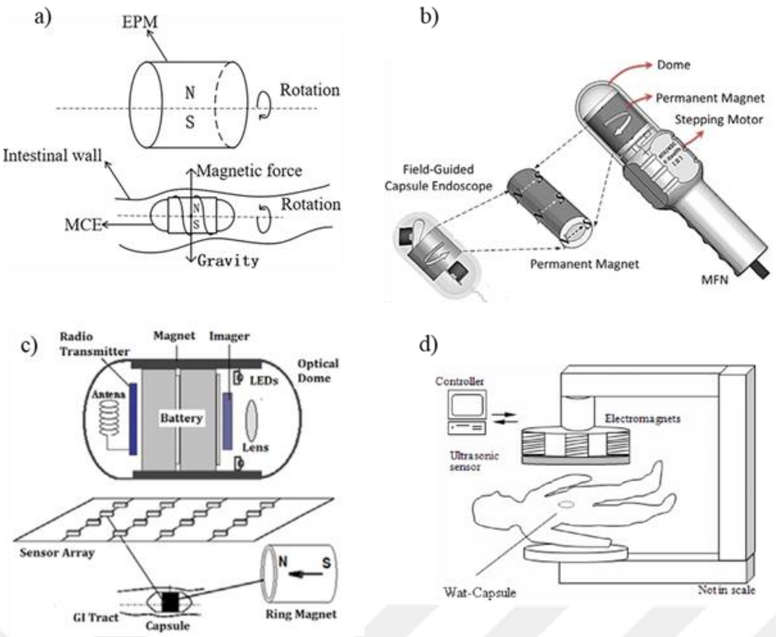

Figure 1.4: a) Image navigation-based closed-loop active control of the magnetic capsule endoscope using a robotic arm [32], b) hand-held magnetic field navigator (MFNs) CE locomotion controller [33], c) Capsule endoscope with ring magnet and sensor array [35], d) a magnetically driven capsule robot is driven by the magnetic field generated by external electromagnets [37].

Apart from the locomotion of the WCE, other studies have been focusing on the development of the capsule’s functionality, such as introducing a tactile sensing mechanism onto the capsules discussed in [39], where a bio-inspired capsule endoscopy (CE) mimics the human-like touch to detect the GI tract lumps. The system relies on the tactile sensor they call Tactip, besides the visual data from the cameras, for the detection of GI abnormalities.

Another study [40] introduces a wireless biopsy method developed on the CE, which is magnetically guided and equipped with thermally responsive microgrippers that fold in response to body temperature and collect tissue samples from the region of interest. The study enables targeted tissue sampling without external tethers. Also, researchers in [41] present a smaller biopsy model integrated with WCE to sample tissues in the small intestine (an inaccessible region). Their model encompasses a rotational razor triggered by a thermal actuator based on paraffin. By getting the signal, the paraffin melts and releases a torsion spring to drive a rotatory blade, which collects superficial abnormal tissues. Besides, for treatment purposes, WCE have been developed in the literature for tasks such as drug delivery. One study [42] presented a drug delivery system using electromagnetic actuation (EMA). The CE developed in the study is equipped with two soft-magnetic rings and a plastic hinge; an external magnetic field guides the capsule through the target tissue, and the magnetic attraction between the rings helps drug extraction. Furthermore, researchers in [43] worked on a micromotor-based drug delivery system that precisely locates and releases drugs on the targeted tissue. Their needle targeting mechanism is capable of rotation and extension, which enables a micro-positioning mechanism and a holding mechanism against natural peristaltic movements of the bowel.

Some of the innovations done in the development of the WCE's functionality are indicated in Figure 1.5.

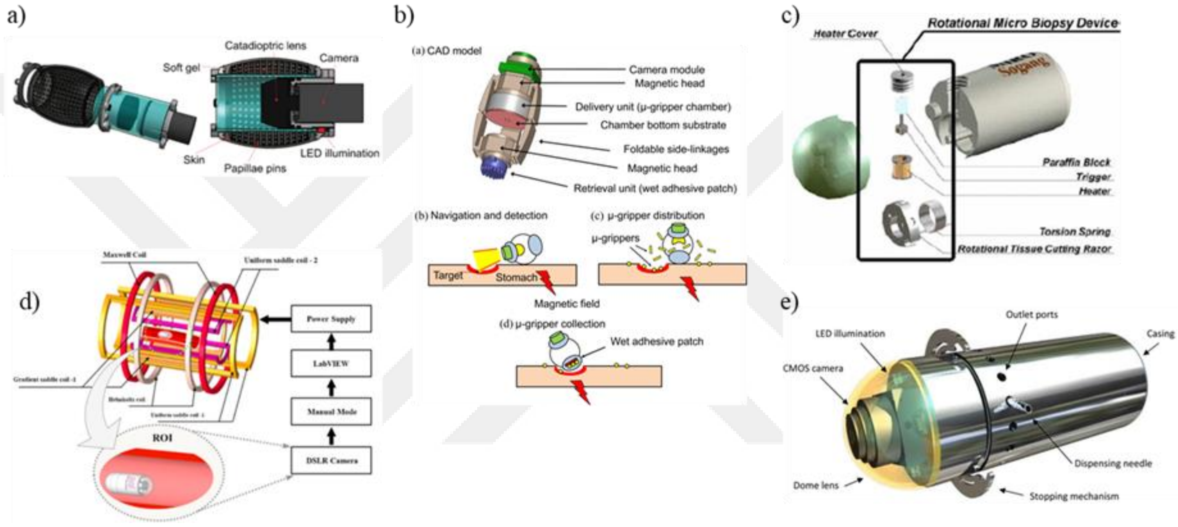

Figure 1.5: Couples of WCE with diverse functionalities discussed: a) Exploded and cross-sectional view of cylindrical Tactip pill design [39], b) Figure representing of a MASCE prototype with the proposed biopsy function [40], c) Rotational micro biopsy WCE [41], d) Diagram of an active locomotive intestinal capsule endoscope that uses electromagnetic actuation to distribute drugs. [42], e) A microrobot concept design capsule endoscopy that can deliver 1 ml of a specific drug while withstanding peristaltic pressure thanks to an inbuilt holding mechanism. [43].

Although several studies have been focusing on the advanced functionality of the WCE, the number of characteristics that can fit into a single capsule is severely constrained by the WCE's small size. The utilization of multiple capsules with combined therapeutic and diagnostic capabilities has been the subject of numerous investigations; these have included methods that concentrate on a magnetic-based self-assembly setup of WCE for modular swallowability [44], allowing for the autonomous connection of individual pill-sized WCE within the GI tract. The design of hermaphrodite mating faces with carefully placed magnets (MASH-1 configuration) is the main technique discussed. Another study [45] focuses on the use of soft magnets whose magnetization direction can be altered by an external electromagnetic actuation (EMA) system. In the process, the drive capsules attach to the functional capsule by magnetic attraction. Lastly two studies have conducted by a team of researchers based on Istanbul Technical University that focused on two methods to accomplish the train like operation of capsules: i) passive control, which involves placing permanent magnets with different orientations on adjacent capsule domes [46], and ii) active control, which involves placing magnet, hall sensor, and coil pairs on adjacent capsules to actively adjust the inter-capsule distance [47]. The magnet-coil illustrated the adoption of the radius of curvature (ROC) as low as 50 mm capabilities for an inter-capsule distance of more than 2 mm, whereas the passive control with two-capsule lead-follow demonstration was limited to a straight path of the GI tract. Stronger magnets and larger currents might be used to further expand the distance between capsules, but doing so would require a significant increase in power consumption.

To create the clinch with a lasso-like throw, this study suggests using spiral springs implanted on the dome areas of the nearby capsules with embedded magnets. Figure 1.6 shows the methods used in approaches [46], [47], and this study.

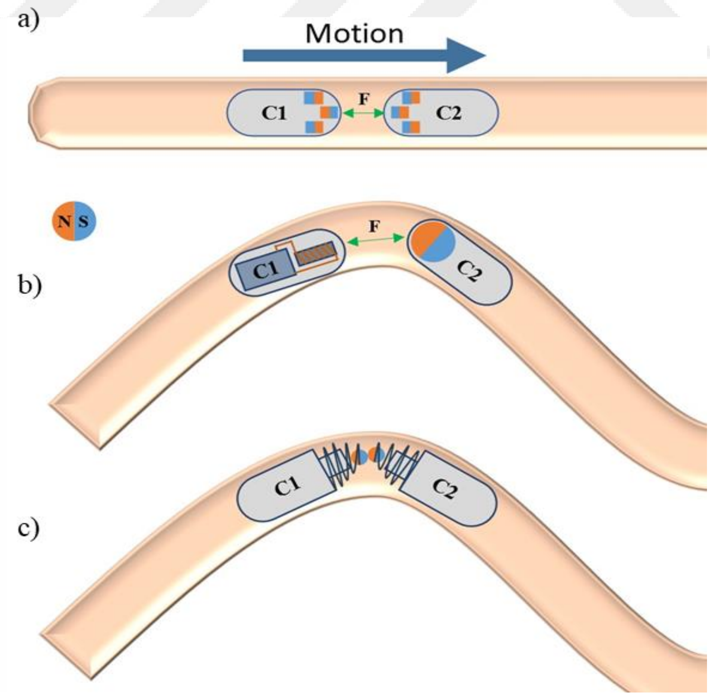

Figure 1.6: Three techniques used in the control of the distance between capsules for multi-capsule endoscopy (a) passive control using magnets [46] (b) active control through the placement of a magnet in one capsule and controlling the coil on the other capsule [47], (c) This work: spring-assisted distance control.

Each capsule in this multi-capsule endoscopy system is equipped with a permanent magnet on the housing unit of the spring. The requirement of the train-like motion of the system is for the capsules to reach the leading capsule, and the passive magnets on each capsule configuration connect to the first capsule swallowed. After the connection, the capsule train will coordinate through the GI tract synchronously with an almost fixed intercapsular distance. In this regard, the overall operation resembles that of a satellite orbiting; without energy consumption, the system moves via the combination of gravitational and centripetal forces. In the case of the capsule endoscope, peristaltic force will move the capsule after the clinch.

1.2 Thesis Outline

This study elaborates in section two on the concept and its methodology by exploring the analytical calculations to restrict spring's streching in order to avoid tissue damage and patient safety, mechanicall modeling of the concept, computer-aided (CAD) designs of the spiral springs, finit element simulations, fabrication process of the capsules, springs, and the intestinal models, experimental setup configuration. Furthermore, motion analysis via MATLAB. Nevertheless, in section three, it indicates the results acquired from different phantoms, such as an ex vivo model, and finally, it shares the concluding remarks and discussion from the proposed study.

2. METHODOLOGY

This study focuses on developing and implementing a spring-assisted, magnetically attached distance management technique for a WCE train, facilitating synchronized traveling of the capsules, especially through curved and twisted paths of the GI tract.

The study involves sequentially the theoretical concept of the work, computational part, design of the model, fabrication process, and experimental tests in which the inter-capsule attachment during the WCE train locomotion, distancing was mimicked, and patient safety was considered by tissue-damage free spring movements.

2.1 Conceptual Framework and Design Objective

This study's main concept is the inter-capsule mechanical connectivity of several WCE using spiral springs equipped with magnets that are fixed to the capsule domes. The objective was to make sure that even when passing over acute intestinal curves, the capsules could keep a constant relative distance during propulsion under peristaltic force.

This was accomplished by designing a spring-magnet system that, when closeness was established, acted as a passive lasso, gripping the trailing capsule. A train-like structure is established through this design that facilitates synchronized movement of the WCEs and improves their locomotion in the digestive system.

The novelty of the concept is due to the use of a passive mechanical compliance, which facilitates peristaltic locomotion without the need for an active onboard actuation.

2.2 Analytical Calculation of Maximum Spring Extension

The first step involved estimating the maximum allowable length for the stretched spring analytically and geometrically. After the physical connection of the WCEs by their spring heads, the springs will stretch and extend during sharp turns of the GI tract to maintain intracapsular connection. The wired connection of the capsules supports the curvature adaptation; besides, it has to guarantee tissue damage-free locomotion due to a potential contact between the springs and the intestinal tissue. As it is shown in Figure 2.1.

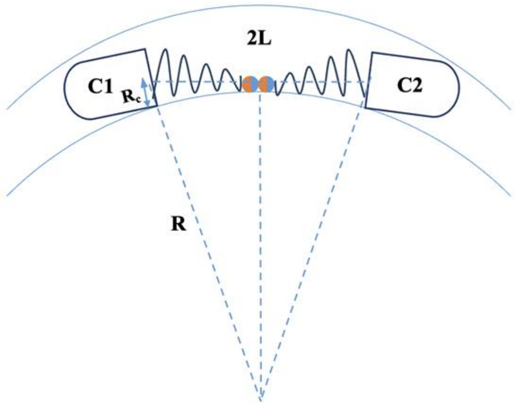

Figure 2.1 : The schematic geometry of the WCE train in a sharp intestinal turn, indicating maximum allowable spring lengths.

If we consider two capsules connected as in Figure 2.1, (R_c) indicates the capsule's diameter and the maximum extended spring length without tissue touch (L), and in a known intestinal curve of (R), it can be written as in equation 2.1;

$$R^2 + L^2 = (R+R_c)^2 \tag{2.1}$$

And the maximum allowable spring length should be considered in the following limit in equation 2.2;

$$L \leq \sqrt{{R_c}^2 + 2R.R_c} \tag{2.2}$$

Considering a minimum radius of curvature as a conservative assumption R=25 mm and a typical capsule radius R_c=6 mm, a safe limit for the maximum extended length L would be L = 18 mm.

This upper limit ensures tissue safety by preventing direct contact between the spring and intestinal walls, particularly in regions with tight curvature. Consequently, it sets a strict design constraint for subsequent spring configurations.

2.3 Modeling

By joining two lumped masses with a spring, as shown in Figure 2.2, spring-connected capsules can be described in both the mechanical and electrical domains to visualize the system's behaviour, including its dynamic behaviour, energy flow, systems response to external disturbances, etc.

When both capsules receive distinct portions of the peristaltic wave, or when there is a disturbance, the spring extends due to the difference in the velocities of the two masses. A model is developed where *m* and *k* are the indication of the capsule's mass and the spring constant. Consequently, the force on capsule 1 (F_1) and capsule 2 (F_2) can be represented as written in equations 2.3 and 2.4.

$$F_1 = m\ddot{x}_1 \tag{2.3}$$

$$F_2 = m\ddot{x}_2 \tag{2.4}$$

In this equation $x_{1,2}$, $\dot{x}_{1,2}$, $\ddot{x}_{1,2}$ ±are the displacement, velocity, and acceleration of capsules 1 and 2, sequentially. The force on the spring (F_k) can be driven by Hook's Law as indicated in equation 2.5;

$$F_k = k_{eff}(x_1 - x_2) \tag{2.5}$$

where k_{eff} = k/2 is the effective spring constant due to the serial connection of two springs. The electric model of equation 2.5 can be rewritten as:

$$V_c = \frac{1}{C}\int i_1 - i_2 \, dt \tag{2.6}$$

where the traditional equivalence between electrical and mechanical components is applied [48].

We model a straightforward situation that makes sense of the experiments that were carried out, in which the leading capsule 1 experiences a constant velocity (A), and the same velocity with an extra time glich is experienced by capsule 2 (called a delta dirac function: δ), which could be brought on by friction, a small jam, or capsules experiencing different peristaltic wave components;

$$\dot{x_1} = A \tag{2.7}$$

$$\dot{x_2} = A + \delta(t - t_0) \tag{2.8}$$

The distance between capsules as a function of time is shown in Figure 2.2c, demonstrating the system's ability to recover even in the presence of the disturbance.

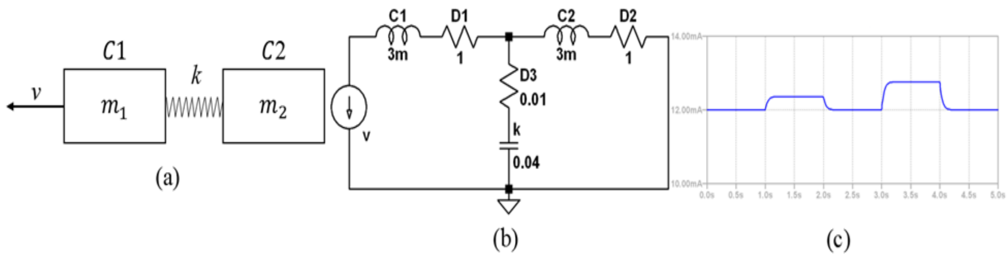

Figure. 2.2: Spring connection between capsules: a) mechanical model, b) circuit model, c) circuit simulation based on the presented model, indicating the distance between capsules in the presence of a perturbation.

2.4 Spring CAD Design

After the attachment of the capsules, they will be moved by peristaltic forces in the GI tract. During some movements, the peristaltic wavelength is smaller than the entire capsule-train length, which may result in experiencing total force just by one capsule. In this way, the spring connection will extend having a stiffness of K (spring constant), with peristaltic force value ($F_{peristalsis}$) of 226 mN [49]. By considering a hemisphere-shaped dome shape of the capsule, spiral springs with various characteristics, such as coil diameter, coil numbers, and lengths, were designed and developed using the SOLIDWORKS CAD software. In the design process, a number of limitations were considered, such as geometrical constraints of the capsule dome, as well as maximum allowable spring extension length and manufacturing conditions such as minimum printable diameter by the printing machine. The spiral spring geometry designed for the study is illustrated in Figure 2.3

Different springs were designed, and every design was tested to evaluate spring characteristics like stiffness (K), stress resistance, and deformation behavior under peristaltic loading circumstances. The spring architecture was constructed on a flat spiral loop in vertical orientation to enhance space efficiency above the semi-spherical dome while preserving structural integrity.

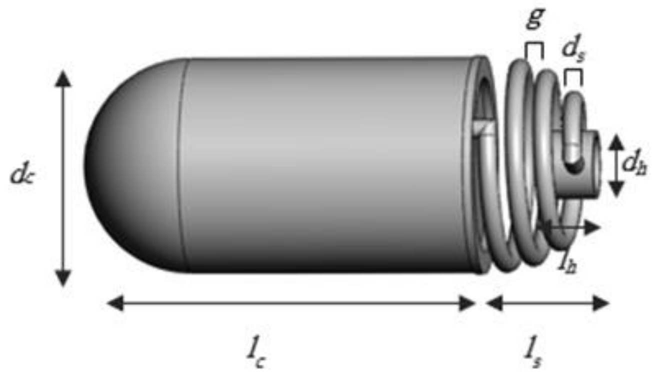

Figure 2.3: A CAD model indicating the spiral spring embedded on the capsule.

The spring's dimensions, which are listed in Table 2.1, were selected based on the capsule dome's dimensions and manufacturing (fused deposition modeling) constraints.

Table 2.1: Spring, capsule dimensions, and material properties.

Parameter	Symbol	Value
Capsule diameter	d_c	12 mm
Capsule length	l_c	26 mm
Spring length	*ls*	6 mm
Spring diameter	d_s	1.1 mm
Spring gap	*g*	1.6 mm
Magnet holder diameter	d_h	2.2 mm
Magnet holder length	l_h	2.4 mm

2.5 Finite Element Modeling and Simulation

The stiffness of a spiral spring with n coils can be modeled as:

$$k = \frac{E}{2(1+\nu)} \frac{d_s^4}{8nd_c^3} \tag{2.9}$$

The values in Table 2.2 are considered, and the geometry of the designed spring, which is illustrated in Figure 2.3, taking n equal to 4, and the average diameter of all four turns of the spring, the spring constant (k) would be approximately k = 45 N/m.

The material property of the Polylactic Acid was used for analytical calculation and defining the spiral springs, which are listed in Table 2.2.

Table 2.2: PLA characteristics [50].

Parameter	Symbol	Value
Young's modulus	E	2.35 GPa
Density	ρ_{pla}	1250 kg/m3
Poisson's ratio	ν	0.33

For further validation of the claims, Finite Element Method (FEM) simulations were conducted to support the analytical evaluation and mechanical performance of each spring design using COMSOL Multiphysics. The simulation process in COMSOL involved using Solid-Mechanics physics and defining the material properties in the first step by referring to PLA's Young's modulus, Poisson's ratio, and Density (Table 1.2) to the designed spring geometry. After that, the base of the spring was constrained to be fixed. The average peristaltic force [49] was applied to the dome of the geometry in the Z direction, mimicking the WCE getting pulled by the leading capsule, which is experiencing the peristaltic contractions in the GI tract. The next step involved assessment of the displacement behaviour of the spring in a given chart, which was used to measure the K constant of the spring analytically by referring to Hooke's law in Equation 2.10. The analysis revealed a spring stiffness of k = 50.9 N/m.

$$F = KX \tag{2.10}$$

Furthermore, COMSOL-based simulations were done to assess other metrics besides the displacement of the springs under peristaltic forces, such as stress distribution under the known forces. After evaluations, the spring constant (k) resulting from analytical evaluations was k≈45N/m, which was in close agreement with the stiffness measured through simulation results, which was measured in COMSOL, k = 50.9 N/m. Both of the measured values remained in allowable error ranges. These outcomes confirmed that the designed spiral springs could sustain physiological forces without breaking down or deformation. Figure 2.4 illustrates a shot from the COMSOL Multiphysics evaluation process.

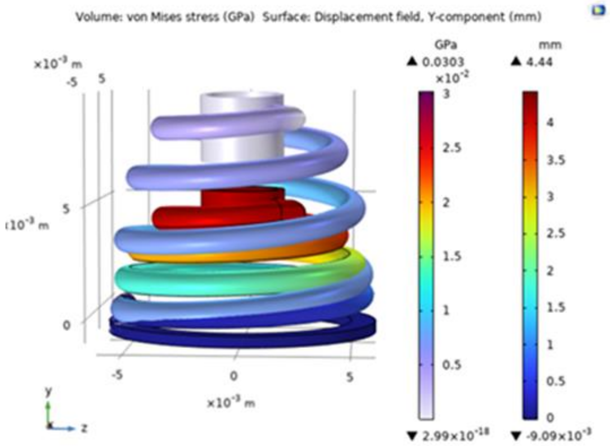

Figure 2.4: Spring evaluation in COMSOL that reveals stress load and displacement under peristaltic force.

2.6 Fabrication via Additive Manufacturing

The next step after designing the various springs and capsules with SolidWorks and validating the design's functionality was printing the spring via fused-deposition modeling using Creality CR-X with a 0.4 mm nozzle and 100% infill, utilizing PLA filaments as shown in Figure 2.5.

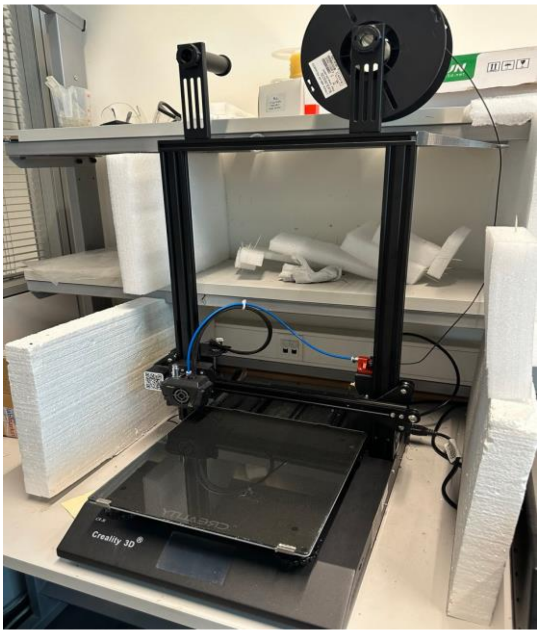

Figure 2.5: 3D printing machine and PLA filament used during the fabrication process

To improve print quality, several fabrication attempts were made, varying support structures, layer resolution, printing temperature, infill density, and print speed. Designs were exported as an STL file and sliced in Cura software. The completed spring measured 6 mm in height, 12 mm in diameter, 1.1 mm in wire diameter, and contained four coils, which were printed in early stages of the experiment. Furthermore, for validating the concept, additionaly two springs with varying metrics (First: 8 number of coils/turns, 12mm height, 12 mm diameter, 1.1 mm wire diameter/ Second: 16 number of coils/turns, 28 mm height, 12 mm diameter, 1.1 mm wire diameter.) were printed. Finally, in order to promote attraction, cylindrical neodymium magnets (2 mm in diameter and 2 mm in height) were placed inside the spring's magnet housings on each capsule.

2.7 Experimental Measurement of Spring Constant

The initial confirmation of the manufactured device's spring constant is conducted using a setup configured specially for displacement behaviour analysis in the laboratory, in which an external camera is used to visualize the spring displacement while applying a specified force amount. And then, the figures achieved during the evaluation tests were assessed by using the ImageJ program for K evaluation. The Spring constant (k) measured in experiments as $k = 40$ N/m, the measured value was consistent with the analytical formulation and in the allowable error range with the finite-element results. The dimensional differences between the manufactured device and the CAD model, as well as the difference between the actual PLA material properties and the simulated values based on measurements in other literature studies, are the reasons attributed to the discrepancy between experimental and simulated values. The setup used for k evaluation included a digital scale for force measurement, a microscope with a camera for tracking the displacement, and a calibrated, precise force-application mechanism. Also, the Hookean behavior was plotted by applying force incrementally while recording displacement. Figure 2.5 is an indication of the setup discussed.

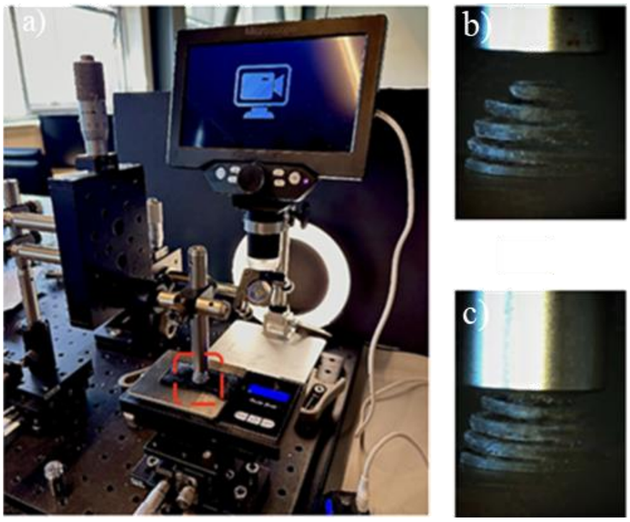

Figure 2.6: Spring Constant test. a) the setup, b) spring without applied force, c) spring with applied force.

2.8 Capsule and Phantom System Preparation

The same PLA material used for spring manufacturing was used to print the capsule bodies, which were also developed in SOLIDWORKS. Several combinations of capsules and springs were put together as illustrated in Figure 2.6:

1. Baseline design was a spring with 4 coils, 6 mm height, and 1.1 mm wire diameter attached to the capsule. 2. The second design was a spring configuration with 12 mm tall, 8 coils, and 1.1 mm wire diameter connected to the capsule body. 3. Finally, the last design was a full spring that encloses the capsule, which had 16 coils, 28 mm height, and 1.1 mm wire thickness.

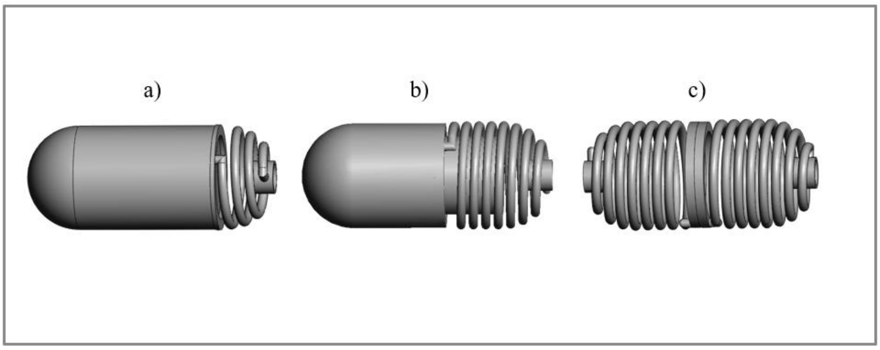

Figure 2.7: Illustration of three varying capsule-spring configurations: a) Baseline design. b) Second design with half spring and capsule, c) final design with full capsule that encloses the capsule.

Additionally, three intestinal phantoms were printed in the study process, respectively, to assess the capsule-train movement:

1. In the early stages of the experiments, intestinal phantoms were made from PLA with two varying radii of curvatures (25 mm and 50 mm) and were implemented in the setup with smoothened surfaces, 2. After gathering expected results from the first bowel models, the next model was made to simulate mucosal compliance, a silicon-coated version of the 25 mm intestinal phantom, 3. Finally, for further validation of the concept, a 3D-printed bowel model (ROC = 25 mm) with actual bovine bowel tissue introduced to its surface was used to mimic the actual GI tract environment.

The different intestinal phantoms are indicated in Figure 2.7.

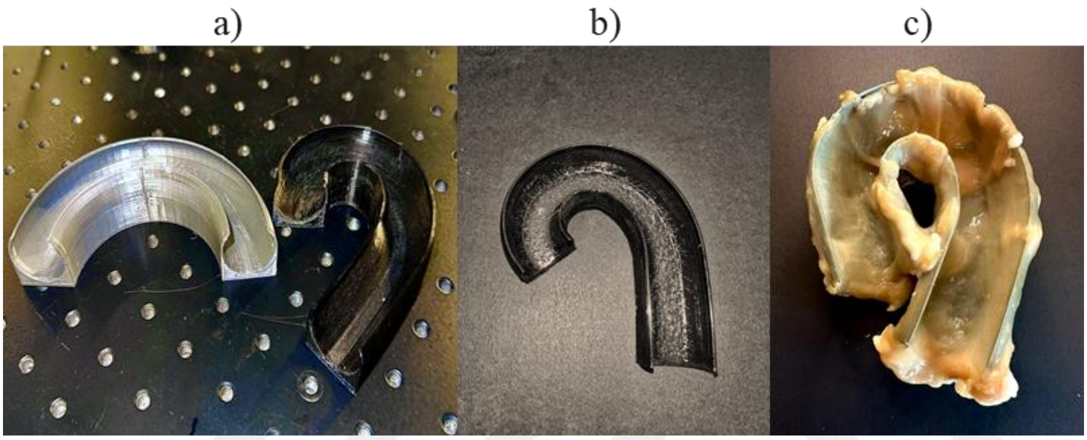

Figure 2.8: Bowel phantoms used during experiments: a) PLA printed, smoothened intestinal phantom with 50 mm and 25 mm ROCs, b) Silicon covered with a villus-like structure, c) Bovine bowel-coated phantom.

2.9 Experimental Setup

Motion control was provided by a motor through a nylon string attached to the front capsule; an Arduino Uno microcontroller interfaced with a PC controlled the stepper motor via the motor driver, moving the nylon string. To imitate accelerated conditions, the translational speed was kept constant at 1 mm/s, around ten times the physiological peristaltic speed [51]. Capsule movement and spacing behaviour of the train, as shown in Figure 2.8 and Figure 2.9, was recorded using an overhead CMOS camera set 0.5 meters above the phantom configuration. Each capsule train in the three separate phantom setups underwent several experimental trials. The trailing capsule's movement, the spring's extension, and the synchronization behavior were all captured during these tests for later analysis.

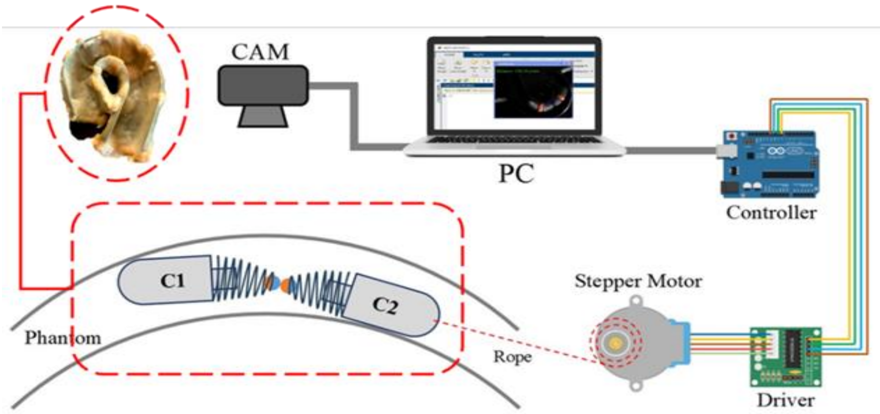

Figure 2.9: A schematic figure of the experimental setup, illustrating the capsule placement in the phantom, the motor, the placement driver, the controller, the PC, and the camera.

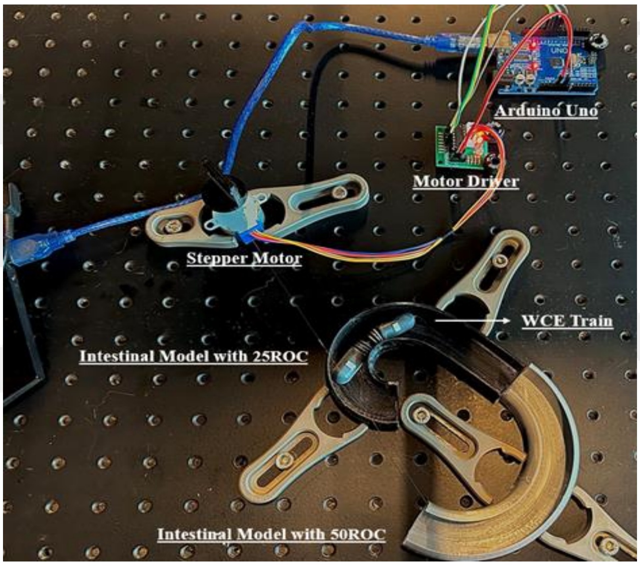

Figure 2.10: A picture from the experimental setup configured in the laboratory.

2.10 Image-Based Motion Analysis

MATLAB-implemented video processing was used to quantitatively assess the capsule train's locomotion and distancing performance. Each capsule was marked with a red tape to aid tracking using an object recognition system based on OpenCV. This program calculated the curved inter-capsule distances as a function of time and determined the centroid positions of the markers. To verify the results, key frames were manually annotated in Fiji (ImageJ) by generating curved distance routes between capsules. Mean inter-capsule distance and displacement variation over time were the two measures recovered. Figure 2.10 shows different shots from video processing on MATLAB.

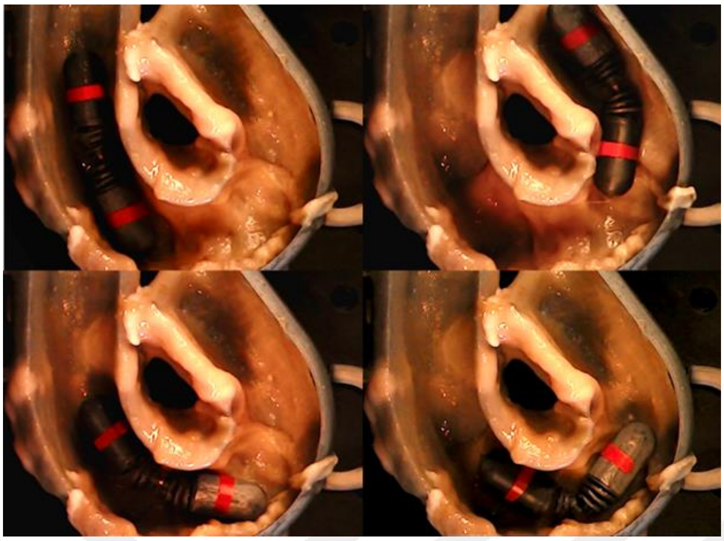

Figure 2.11: Screenshot from the experiment video from which the inter-capsule distance was monitored via a CMOS camera.

3. RESULTS

To examine the efficiency of the proposed method of spring-assisted distance management of the WCE train, a couple of ex-vivo experiments were conducted. Capsule springs configuration equipped with neodymium magnets were implemented into a phantom illustrating an intestinal environment, specifically, a bovine colon attached to a radius-of-curvature conduit of 25 mm. The follower capsule was engaged by spring clinching, mimicking in vivo peristaltic-driven motion, while the leading capsule was pulled at a controlled speed of 1 mm/s.

Thin red tapes were stuck to the capsule surfaces, and a CMOS camera placed above the experimental setup was used to track the capsule positions in order to make further measurements of the inter-capsule distance. Image processing was done using a motion examining MATLAB module built on the OpenCV library; validation of the module was done manually on the image analysis tool FIJI. Measurements along the intestinal phantom for both direct (beeline) and adjusted curved distances guaranteed the quality and authenticity of the findings.

The average inter-capsular distance, measured based on the distance between red tapes, was calculated as 2L = 24.5. This amount is a bit shorter than the expected value from theoretical calculations under the average peristaltic force of 226 mN [49]. The lower forces in the experimental setup, such as frictional contacts between the capsules and the phantom surface, and the substitution of a motor-driven, controlled pulling mechanism for actual peristaltic pressure, are the main reasons for the majority of this difference. For exploring the impact of the spring stiffness on the WCE train (Table 3.1), three varying capsule-spring configurations, as mentioned in section 2.7, were designed and fabricated with approximately half and one quarter of the first spring stiffness (K) value. As illustrated in Figure 3.1, the configurations encompassing the lower stiffnesses exhibited a bigger inter-capsule distance. These results indicate that reduced spring stiffness permits greater extension without compromising the structural connection between the capsules.

The graph indicates that by lowering stiffness, the intercapsular distance increases. However, in quarter stiffness spring due to the fabrication technique, which involved sticking two half springs together by glue, the pulling force only affected the leading spring, so that its distancing behaviour did not vary as expected.

All things considered, the results show that spring-assisted clinching successfully preserves a constant inter-capsule distance even in the minimum radius of curvature (ROC = 25 mm) of the GI tract. This challenge in studies in the literature based on magnet-coil and non-contact magnetic coupling systems was found difficult to overcome. Additionally, the spring design prevented accidental contact with the intestinal wall by consistently limiting capsule extension within the specified safety margins.

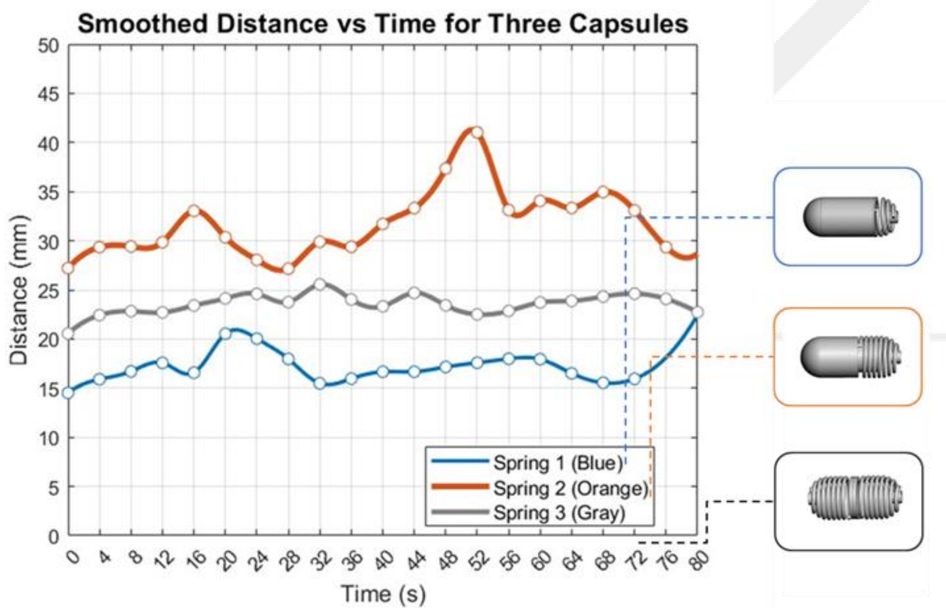

Figure 3.1: Inter-capsule distance vs. time observed for three different springs integrated on capsules.

Table 3.1: Average inter-capsule distances for different spring designs.

Spring Type	Spring Constant (N/m)	Average Interscapular Distance (mm)
Stiff spring (initial design)	*40*	24.5
Half-stiffness spring	~20	24.8
Quarter-stiffness spring	~10	25.0

By comparing the proposed technique with earlier approaches that used passive magnets [46] and an active magnetic system [47], this system demonstrates improved flexibility in tight curves and maintains an optimal distance without capsule detachment throughout the entire motion. Table 3.2 compares these three approaches.

Table 3.2: Comparison of two earlier approaches with the technique proposed in this study.

Feature	Spring-Assisted	Passive magnetic System	Active Magnetic System
ROC limit	25 mm	100 mm	50 mm
Energy Consumption	Low	Low	High
Attachment stability	High	Very low	Low

4. DISCUSSION

This study focused on a new approach to distance management between WCEs in a capsule train by introducing a spring-assisted magnetic attachment of the multi-capsule endoscopy train. The technique was developed mainly to address a previously discussed challenge in the literature by either the passive magnetic connections or active magnet-coil mechanism of the WCE train, which had the main drawbacks of passing through sharp turns of the GI tract, adapting to tight curves, and high energy consumption during its locomotion.

The findings demonstrated that a magnet-equipped spiral spring that attaches to the capsule's dome was a good solution for addressing the capsule connectivity in every path by offering a compatible and energy-efficient connection to the train. A synchronized movement of the WCE train is established after the physical engagement of two springs through their magnet assemblies, which provides a stable and flexible connection through the sharpest bends in the GI tract with a radius of curvature as small as 25mm. The spring-assisted method provides significant improvements in curvature adaptability without a continuous input energy requirement, in contrast to previous passive magnetic approaches that were mostly limited to straight pathways or active coil-magnet systems that were performed only in ROCs no smaller than 50 mm.

The spring design was optimized through the use of finite element simulations in conjunction with analytical computations. To avoid unintended tissue damage to the intestinal wall, the maximum allowable spring extension was carefully calculated, ensuring patient safety during the operation. The spring constant's experimental validation nearly matched the theoretical predictions, with only modest variations explained by manufacturing errors and material heterogeneity in the 3D-printed PLA structures. Such small variations were not discovered to affect the mechanical performance of the spring under simulated peristaltic circumstances and are to be anticipated in practical implementations.

For further validation of the system's robustness, extra experiments with various spring stiffnesses were conducted. These tests confirmed that even with the variations in spring stiffness, the inter-capsule distance remains within the safe and functional expected limit, with an average distance ranging between 24.5 mm and 25 mm. These findings imply that adjusting the spring stiffness provides design freedom, hence allowing the system to be fitted to various patient anatomies or clinical situations.

Nevertheless, a couple of restrictions were noticed, such as the motor-driven pulling system used in the experiment is helpful for reproducible testing, but it falls short of accurately simulating the complex and variable forces involved in actual peristaltic movement. The variations observed between theoretical and experimental inter-capsule distances can be addressed by the friction between the capsules' bodies and the phantom models, as well as the difference in motion dynamics. Furthermore, even though the spring mechanism was successful in enabling clinching and preserving capsule connectivity, the open spring structure design may expose biological surroundings to internal capsule components. Also, in this study, we focused only on single-stretch deformation and did not consider plastic deformation, which may occur after several uses. For further study, cyclic mechanical fatigue tests, such as deformation tests, will be considered, and a biocompatible protective cover could be incorporated into future versions of this design to safeguard internal components and guarantee long-term operating stability.

In addition, another important requirement to be considered for the WCE train is the development of an active navigation system so that the magnets can get clinched in the GI tract. Although this study mostly addressed the attachment method, future work has to combine or create compatible locomotion strategies to allow completely autonomous capsule train assembly inside the GI tract.

In conclusion, the spring-assisted capsule endoscopy train connection technique presented in this work shows a potential path for improving multi-capsule endoscopic capacity. Its capacity to preserve capsule alignment over acute bends without constant energy use shows a major improvement over earlier described techniques. This approach offers great promise to assist next-generation diagnostic and therapeutic capsule systems with more refinement, including better encapsulation and integrated navigation solutions.

REFERENCES

[1] **Basil Akpunonu, Jeannine Hummell, Joseph D. Akpunonu, Shahab Ud Din.** Capsule endoscopy in gastrointestinal disease: Evaluation, diagnosis, and treatment. Cleveland Clinic Journal of Medicine Apr 2022, 89 (4) 200-211; DOI: 10.3949/ccjm.89a.20061

[2] **Prabakaran, Prashanth & Guda, Nalini & Thomas, Jacob & Heise, Charles & Gopal, Deepak.** (2019). Clinical approach to obscure GI bleeding - Diagnostic testing and management. Journal of Digestive Endoscopy. 4. 61. 10.4103/0976-5042.129966.

[3] **Yun, S., Kim, K., & Nam, S.** (2010). Outer-Wall Loop Antenna for Ultrawideband Capsule Endoscope System. IEEE Antennas and Wireless Propagation Letters, 9, 1135-1138. https://doi.org/10.1109/LAWP.2010.2094996

[4] **Faerber, J., Cummins, G., Pavuluri, S. K., Record, P., Rodriguez, A. R. A., Lay, H. S., McPhillips, R., Cox, B. F., Connor, C., Gregson, R., Clutton, R. E., Khan, S. R., Cochran, S., & Desmulliez, M. P. Y.** (2018). In Vivo Characterization of a Wireless Telemetry Module for a Capsule Endoscopy System Utilizing a Conformal Antenna. IEEE Transactions on Biomedical Circuits and Systems, 12(1), 95-105. https://doi.org/10.1109/TBCAS.2017.2759254

[5] **Hintea, S., Simion, E., & Festila, L.** (1996). Radio frequency link used in partially-implanted auditory prosthesis. Proceedings of Third International Conference on Electronics, Circuits, and Systems, 2, 1143-1146 c.2. https://doi.org/10.1109/ICECS.1996.584624 .

[6] **Höög, C., Bark, L.-Å., Arkani, J., Gorsetman, J., Broström, O., & Sjöqvist, U.** (2012). Capsule Retentions and Incomplete Capsule Endoscopy Examinations: An Analysis of 2300 Examinations. Gastroenterology research and practice, 2012, 518718. https://doi.org/10.1155/2012/518718ASTM standards on geosynthetics. (2000). West Conshohocken, Penn: ASTM.

[7] **Catania, A., Mariani, S., D'Onofrio, M., Silvani, M., & Menciassi, A.** (2025). *In vivo validation of wireless power transfer system for magnetically controlled robotic capsule endoscopy*. arXiv. https://arxiv.org/abs/2503.12850

[8] **Nia, G. J., Maleki, M., Khalilzadeh, M., & Amini, N.** (2024). An overview of emerging smart capsules using other-than-light technologies for colonic disease detection. *Diagnostics*, *14*(5), 512. https://doi.org/10.3390/diagnostics14050512

[9] **Cheung, E., Karagozler, M. E., Park, S., Kim, B., & Sitti, M.** (2005). A new endoscopic microcapsule robot using beetle inspired microfibrillar adhesives. Proceedings, 2005 IEEE/ASME International Conference on Advanced Intelligent Mechatronics., 551-557. https://doi.org/10.1109/AIM.2005.1511040

[10] **Hosokawa, D., Ishikawa, T., Morikawa, H., Imai, Y., & Yamaguchi, T.** (2009). A Locomotive System Mimicking Pedal Locomotion of Snails for the Capsule Endoscope. In: Vander Sloten, J., Verdonck, P., Nyssen, M., Haueisen, J. (eds) 4th European Conference of the International Federation for Medical and Biological Engineering. IFMBE Proceedings, vol 22. Springer, Berlin, Heidelberg. https://doi.org/10.1007/978-3-540-89208-3_393

[11] **Hosokawa, D., Ishikawa, T., Morikawa, H., Imai, Y., & Yamaguchi, T.** (2009). Development of a biologically inspired locomotion system for a capsule endoscope. The International Journal of Medical Robotics and Computer Assisted Surgery, 5(4), 471-478. https://doi.org/https://doi.org/10.1002/rcs.284

[12] **Kim, B., Park, S., Jee, C. Y., & Yoon, S.-J**. (2005). An earthworm-like locomotive mechanism for capsule endoscopes. 2005 IEEE/RSJ International Conference on Intelligent Robots and Systems, 2997-3002. https://doi.org/10.1109/IROS.2005.1545608

[13] **Kim, B., Park, S., & Park, J.-O.** (2009). Microrobots for a capsule endoscope. 2009 IEEE/ASME International Conference on Advanced Intelligent Mechatronics, 729-734. https://doi.org/10.1109/AIM.2009.5229926 Columbia University, Teachers College, Institute for Learning Technologies. (2000). Smart cities: New York: Electronic education for the new millennium [PowerPoint slides]. Retrieved from http://www.ilt.columbia.edu/publications/index.html

[14] **Kwon, J., Park, S., Park, J., & Kim, B.** (2007). Evaluation of the critical stroke of an earthworm-like robot for capsule endoscopes. Proceedings of the Institution of Mechanical Engineers, Part H: Journal of Engineering in Medicine, 221(4), 397-405. https://doi.org/10.1243/09544119JEIM134

[15] **Kim, B., Lee, S., Park, J. H., & Park, J.-O.** (2005). Design and fabrication of a locomotive mechanism for capsule-type endoscopes using shape memory alloys (SMAs). IEEE/ASME Transactions on Mechatronics, 10(1), 77-86. https://doi.org/10.1109/TMECH.2004.842222.

[16] **Kim, H. M., Yang, S., Kim, J., Park, S., Cho, J. H., Park, J. Y., Kim, T. S., Yoon, E.-S., Song, S. Y., & Bang, S.** (2010). Active locomotion of a

paddling-based capsule endoscope in an in vitro and in vivo experiment (with videos). Gastrointestinal Endoscopy, 72(2), 381-387. https://doi.org/https://doi.org/10.1016/j.gie.2009.12.058

[17] **Yang, S., Park, K., Kim, J., Kim, T. S., Cho, I.-J., & Yoon, E.-S.** (2011). Autonomous locomotion of capsule endoscope in the gastrointestinal tract. 2011 Annual International Conference of the IEEE Engineering in Medicine and Biology Society, 6659-6663. https://doi.org/10.1109/IEMBS.2011.6091642

[18] **Park, H., Park, S., Yoon, E., Kim, B., Park, J., & Park, S.** (2007). Paddling-based Microrobot for Capsule Endoscopes. Proceedings 2007 IEEE International Conference on Robotics and Automation, 3377-3382. https://doi.org/10.1109/ROBOT.2007.363994

[19] **Valdastri, P., Webster, R. J., Quaglia, C., Quirini, M., Menciassi, A., & Dario, P.** (2009). A New Mechanism for Mesoscale Legged Locomotion in Compliant Tubular Environments. IEEE Transactions on Robotics, 25(5), 1047-1057. https://doi.org/10.1109/TRO.2009.2014127

[20] **Li, W. D., Guo, W., Li, M. T., & Zhu, Y. H.** (2006). Design and Test of a Capsule-Type Endoscope Robot with Novel Locomotion Principle. 2006 9th International Conference on Control, Automation, Robotics and Vision, 1-6. https://doi.org/10.1109/ICARCV.2006.345240

[21] **Liu, L., Towfighian, S., & Hila, A.** (2015). A Review of Locomotion Systems for Capsule Endoscopy. IEEE Reviews in Biomedical Engineering, 8, 138-151. https://doi.org/10.1109/RBME.2015.2451031

[22] **Sliker, L. J., Kern, M. D., & Rentschler, M. E.** (2013). Preliminary experimental results and modeling for a four-degree-of-freedom automated traction measurement platform for quantitative evaluation of in vivo robotic capsule colonoscopy mobility effectiveness. 2013 IEEE International Conference on Robotics and Automation, 4875-4880. https://doi.org/10.1109/ICRA.2013.6631273

[23] **Terry, B. S., Passernig, A. C., Hill, M. L., Schoen, J. A., & Rentschler, M. E.** (2012). Small intestine mucosal adhesivity to in vivo capsule robot materials. Journal of the Mechanical Behavior of Biomedical Materials, 15, 24-32. https://doi.org/https://doi.org/10.1016/j.jmbbm.2012.06.018

[24] **Sliker, L. J., Schoen, J. A., & Rentschler, M. E.** (2010). Preliminary in vivo capsule crawler mobility. In International Design Engineering Technical Conferences and Computers and Information in Engineering Conference (Vol. 44106, pp. 135-144).

[25] **Karagozler, M. E., Cheung, E., Kwon, J., & Sitti, M.** (2006). Miniature Endoscopic Capsule Robot using Biomimetic Micro-Patterned Adhesives. The First IEEE/RAS-EMBS International Conference on Biomedical

Robotics and Biomechatronics, 2006. BioRob 2006., 105-111. https://doi.org/10.1109/BIOROB.2006.1639068

[26] **Chen, J., Zhu, X., & Qiu, C.** (2009). Locomotion and steering design of an active capsule robot for endoscopic inspection. 2009 IEEE International Conference on Robotics and Biomimetics (ROBIO), 2344-2348. https://doi.org/10.1109/ROBIO.2009.5420751

[27] **Liang, H., Guan, Y., Xiao, Z., Hu, C., & Liu, Z.** (2011). A screw propelling capsule robot**.** 2011 IEEE International Conference on Information and Automation, 786-791. https://doi.org/10.1109/ICINFA.2011.5949101

[28] **Carta, R., Tortora, G., Thoné, J., Lenaerts, B., Valdastri, P., Menciassi, A., Dario, P., & Puers, R.** (2009). Wireless powering for a self-propelled and steerable endoscopic capsule for stomach inspection. Biosensors and Bioelectronics, 25(4), 845-851. https://doi.org/https://doi.org/10.1016/j.bios.2009.08.049

[29] **Falco, I. De, Tortora, G., Dario, P., & Menciassi, A.** (2014). An Integrated System for Wireless Capsule Endoscopy in a Liquid-Distended Stomach. IEEE Transactions on Biomedical Engineering, 61(3), 794-804. https://doi.org/10.1109/TBME.2013.2290018

[30] **Carta, R., Sfakiotakis, M., Pateromichelakis, N., Thoné, J., Tsakiris, D. P., & Puers, R.** (2011). A multi-coil inductive powering system for an endoscopic capsule with vibratory actuation. Sensors and Actuators A: Physical, 172(1), 253-258. https://doi.org/https://doi.org/10.1016/j.sna.2011.03.036

[31] **Oh DJ, Kim KS, Lim YJ**. A New Active Locomotion Capsule Endoscopy under Magnetic Control and Automated Reading Program. Clin Endosc. 2020;53(4):395-401. doi: 10.5946/ce.2020.127

[32] **Bo Ye, Yingbing Fu, Shicong Zhang, Hao Wang, Guo Fang, Wei Zha, Amit Krishna Dwivedi,** Closed-loop active control of the magnetic capsule endoscope with a robotic arm based on image navigation, Journal of Magnetism and Magnetic Materials, Volume 565, 2023, 170268, ISSN 0304-8853,**https://doi.org/10.1016/j.jmmm.2022.170268.**

[33] **G. -S. Lien, C. -W. Liu, J. -A. Jiang, C. -L. Chuang and M. -T. Teng,** "Magnetic Control System Targeted for Capsule Endoscopic Operations in the Stomach—Design, Fabrication, and in vitro and ex vivo Evaluations," in *IEEE Transactions on Biomedical Engineering*, vol. 59, no. 7, pp. 2068-2079, July 2012, https://doi.org/10.1109/TBME.2012.2198061

[34] **Rahman, I., Pioche, M., Shim, C. S., Lee, S. P., Sung, I.-K., Saurin, J.-C., & Patel, P.** (2016). Magnetic-assisted capsule endoscopy in the upper GI tract by using a novel navigation system (with video). Gastrointestinal Endoscopy, 83(5), 889-895.e1. https://doi.org/https://doi.org/10.1016/j.gie.2015.09.015

[35] **Hu, C., Ren, Y., You, X., Yang, W., Song, S., Xiang, S., He, X., Zhang, Z., & Meng, M. Q. .-H.** (2016). Locating Intra-Body Capsule Object by Three-Magnet Sensing System. IEEE Sensors Journal, 16(13), 5167-5176. https://doi.org/10.1109/JSEN.2016.2558198

[36] **Hoang, M. C., Nguyen, K. T., Le, V. H., Kim, J., Choi, E., Kang, B., Park, J.-O., & Kim, C.-S**. (2021). Independent Electromagnetic Field Control for Practical Approach to Actively Locomotive Wireless Capsule Endoscope. IEEE Transactions on Systems, Man, and Cybernetics: Systems, 51(5), 3040-3052. https://doi.org/10.1109/TSMC.2019.2917298

[37] **Hosseini, S., & Khamesee, M. B.** (2009). Design and control of a magnetically driven capsule-robot for endoscopy and drug delivery. 2009 IEEE Toronto International Conference Science and Technology for Humanity (TIC-STH), 697-702. https://doi.org/10.1109/TIC-STH.2009.5444409

[38] **F. N. Alsunaydih, J. -M. Redouté and M. R. Yuce**, "A Locomotion Control Platform With Dynamic Electromagnetic Field for Active Capsule Endoscopy," in IEEE Journal of Translational Engineering in Health and Medicine, vol. 6, pp. 1-10, 2018, Art no. 1800710, doi:10.1109/JTEHM.2018.2837895.

[39] **Camboni D, Massari L, Chiurazzi M, et al** (2021) Endoscopic Tactile Capsule for Non-Polypoid Colorectal Tumour Detection. IEEE Trans Med Robot Bionics 3:. https://doi.org/10.1109/TMRB.2020.3037255

[40] **Yim S, Gultepe E, Gracias DH, Sitti M** (2014) Biopsy using a magnetic capsule endoscope carrying, releasing, and retrieving untethered microgrippers. IEEE Trans Biomed Eng 61:. https://doi.org/10.1109/TBME.2013.2283369

[41] **Kong KC, Cha J, Jeon D, Cho DID** (2005) A rotational micro biopsy device for the capsule endoscope. In: 2005 IEEE/RSJ International Conference on Intelligent Robots and Systems, IROS

[42] **Le VH, Rodriguez HL, Lee C, et al** (2016) A soft-magnet-based drug-delivery module for active locomotive intestinal capsule endoscopy using an electromagnetic actuation system. Sens Actuators A Phys 243:. https://doi.org/10.1016/j.sna.2016.03.020

[43] **S. P. Woods and T. G. Constandinou**, "Wireless Capsule Endoscope for Targeted Drug Delivery: Mechanics and Design Considerations," in IEEE Transactions on Biomedical Engineering, vol. 60, no. 4, pp. 945-953, April 2013, doi: 10.1109/TBME.2012.2228647

[44] **Z. Nagy, R. Oung, J. J. Abbott and B. J. Nelson**, "Experimental investigation of magnetic self-assembly for swallowable modular robots," 2008 IEEE/RSJ International Conference on Intelligent Robots and Systems, Nice, France, 2008, pp. 1915-1920, doi: 10.1109/IROS.2008.4650662.

[45] **Li Z, Hoang MC, Kim CS, et al** (2021) Modular capsules with assembly and separation mechanism: Proof of concept. Actuators 10:. https://doi.org/10.3390/act10070159

[46] **Peker F, Ferhanoğlu O** (2021) Multi-Capsule Endoscopy: An initial study on modeling and phantom experimentation of a magnetic capsule train. J Med Biol Eng 41:. https://doi.org/10.1007/s40846-021-00610-6

[47] **Peker F, Ferhanoğlu O** (2024) Active distance control in multi-capsule endoscopy via closed loop electromagnetic force between capsules. Med Biol Eng Comput 62:. https://doi.org/10.1007/s11517-023-02997-7

[48] **Senturia SD** (2001) Microsystem Design

[49] **Rehan M, Al-Bahadly I, Thomas DG, Avci E** (2021) Measurement of peristaltic forces exerted by living intestine on robotic capsule. IEEE/ASME Transactions on Mechatronics 26:. https://doi.org/10.1109/TMECH.2021.3078139

[50] **Kamer MS, Temiz Ş, YAYKAŞLI H, et al** (2022) EFFECT OF PRINTING SPEED ON FDM 3D-PRINTED PLA SAMPLES PRODUCED USING DIFFERENT TWO PRINTERS. International Journal of 3D Printing Technologies and Digital Industry 6:. https://doi.org/10.46519/ij3dptdi.108880

[51] **Freitas M, Silva VM, Xavier S, et al** (2023) Prolonged Gastric Transit Time in Small-Bowel Capsule Endoscopy: Which Patients Are at Risk and What Are the Implications? Turkish Journal of Gastroenterology 34:. https://doi.org/10.5152/tjg.2023.22191

[52] **Li, H., Yi, X., Zhang, Z., & Chen, Y.** (2024). Magnetic-Controlled Microrobot: Real-Time Detection and Tracking through Deep Learning Approaches. Micromachines, 15(6),756:. https://doi.org/10.3390/mi15060756

[53] **Jiayi Huo, Jiaying He, Jiayao Zhou, Bo Yuan, Xuxiang Ni, Liqiang Wang,** Three-dimensional endoscopic imaging system based on micro-lithography mask structured light projection, Optics Communications, Volume 575,2025,131295, ISSN 0030-4018, https://doi.org/10.1016/j.optcom.2024.131295.

[54] **Singeap A-M, Sfarti C, Minea H, Chiriac S, Cuciureanu T, Nastasa R, Stanciu C, Trifan A.** Small Bowel Capsule Endoscopy and Enteroscopy: A Shoulder-to-Shoulder Race. Journal of Clinical Medicine. 2023; 12(23):7328. https://doi.org/10.3390/jcm12237328

[55] **Smith J.** Advances in capsule endoscopy for small bowel diagnostics. Gastroenterology & Endoscopy News [Internet]. 2025 [cited 2025 May 18]; Available from: https://www.gastroendonews.com/In-the-News/Article/05-25/Advances-in-Capsule-Endoscopy-for-Small-Bowel-Diagnostics/12345

APPENDICES

APPENDIX A: Visual tracking codes on MATLAB
APPENDIX B: Arduino Uno code
APPENDIX C: CAD designs

APPENDIX A: Matlab Video tracking code:

```
% Load video

videoFile = 'D:\1.mp4'; % Change this to your actual video filename
video = VideoReader(videoFile);

% Create a VideoWriter for the output video
outputVideo = VideoWriter('output_with_distance.mp4', 'MPEG-4');
outputVideo.FrameRate = video.FrameRate;
open(outputVideo);

% Initialize variables
frameRate = video.FrameRate;
numFrames = floor(video.Duration * frameRate);
time = (0:numFrames-1) / frameRate;
distances_pixels = nan(1, numFrames);
curved_distances_mm = nan(1, numFrames); % Store actual curved distances

prevCenters = []; % To track previous positions of the labels

% Constants
real_distance_m = 0.026; % 26mm = 0.026m for scaling
R = 25; % mm (radius of curvature in curved region)
curve_duration = 35; % Duration in seconds before the path straightens

% Create a figure for displaying video frames
figure;
hold on;

% Process each frame
for k = 1:numFrames
    frame = read(video, k);

    % Convert frame to HSV for better color detection
    hsvFrame = rgb2hsv(frame);

    % Define red color threshold
    redMask = ( (hsvFrame(:,:,1) > 0.95 | hsvFrame(:,:,1) < 0.05) & ...
                (hsvFrame(:,:,2) > 0.6) & ...
                (hsvFrame(:,:,3) > 0.4) );

    % Perform morphological operations to clean up noise
    redMask = imopen(redMask, strel('disk', 5)); % Reduce small noise
    redMask = imclose(redMask, strel('disk', 7)); % Fill gaps in labels
    redMask = imfill(redMask, 'holes'); % Fill any remaining holes

    % Detect red regions
    stats = regionprops(redMask, 'Centroid', 'Area');

    % Only consider large enough areas to avoid noise
    minAreaThreshold = 50;
    stats = stats([stats.Area] > minAreaThreshold);

    if length(stats) >= 2
        % Extract centroids
        centers = cat(1, stats.Centroid);
```

```
        % Assign labels based on previous frame positions
        if isempty(prevCenters)
            centers = sortrows(centers, 1); % Sort by x-coordinates
initially
        elseif size(centers, 1) == 2 && size(prevCenters, 1) == 2
            % Find the closest match to previous positions
            dists = vecnorm(centers - prevCenters, 2, 2);
            [~, idx] = sort(dists);
            centers = centers(idx(1:2), :);
        end

        % Compute Euclidean distance between the two label centers (in
pixels)
        newDistance = sqrt(sum((centers(2,:) - centers(1,:)).^2));

        % Outlier rejection (if change > 5 pixels from previous frame,
discard)
        if k > 1 && abs(newDistance - distances_pixels(k-1)) > 5
            distances_pixels(k) = distances_pixels(k-1);
        else
            distances_pixels(k) = newDistance;
            prevCenters = centers; % Update previous positions
        end

        % Convert pixel distances to real-world distances (mm)
        initial_distance_pixels = distances_pixels(1);
        scale_factor = real_distance_m / initial_distance_pixels;
        d_mm = distances_pixels(k) * scale_factor * 1000; % Convert to mm

        % Adjust for curvature during the first 35 seconds
        if time(k) <= curve_duration
            if d_mm < 2 * R  % Ensure valid range for arcsin
                theta = 2 * asin(d_mm / (2 * R)); % Compute central angle
                curved_distances_mm(k) = R * theta; % Compute arc length
            else
                curved_distances_mm(k) = d_mm; % If d_mm is too large,
fallback to straight-line
            end
        else
            curved_distances_mm(k) = d_mm; % Straight path, no curvature
correction
        end

        % Overlay distance on the frame
        frameWithText = insertText(frame, [10, 30], ...
            sprintf('Distance: %.2f mm', curved_distances_mm(k)), ...
            'FontSize', 30, 'TextColor', 'green', 'BoxColor', 'black');

        % Draw bounding boxes around detected labels
        for i = 1:2
            frameWithText = insertShape(frameWithText, 'Rectangle', ...
                [centers(i,1)-10, centers(i,2)-10, 20, 20], 'Color',
'green', 'LineWidth', 2);
        end

        % Draw a line connecting the two detected labels
        frameWithText = insertShape(frameWithText, 'Line', ...
```

```
            [centers(1,1), centers(1,2), centers(2,1), centers(2,2)],
'Color', 'blue', 'LineWidth', 2);
    else
        frameWithText = frame; % If detection fails, just keep the frame
    end

    % Display the processed frame
    imshow(frameWithText);
    drawnow;

    % Write the processed frame to the output video
    writeVideo(outputVideo, frameWithText);
end

% Close the output video writer
close(outputVideo);
disp('Video processing complete! Saved as output_with_distance.mp4');

%% Data Processing: Convert to Real Distance and Plot

% Handle missing (NaN) values by interpolation
curved_distances_mm = fillmissing(curved_distances_mm, 'linear');

% Smooth the data using Savitzky-Golay filter for better continuity
curved_distances_mm = smoothdata(curved_distances_mm, 'sgolay', 11);  %
You can try 'lowess' too

% Filter out distances that are unrealistically small (<26 mm)
curved_distances_mm(curved_distances_mm < 26) = NaN;

% Plot displacement vs. time (in mm)
figure;
plot(time, curved_distances_mm, 'r-', 'LineWidth', 2);
xlabel('Time (s)', 'FontSize', 12);
ylabel('Distance between labels (mm)', 'FontSize', 12);
title('Smoothed Displacement between Red Labels Over Time', 'FontSize',
14);
ylim([0 60]); % Set Y-axis limits between 0 and 60 mm
grid on;
```

APPENDIX B: Stepper Motor Control via Arduino Uno

```
#include <Stepper.h>

// Constants
const int stepsPerRevolution = 2048; // Full revolution for 28BYJ-48
stepper
const float pulleyDiameter = 2.55;   // Pulley diameter in cm
const float pulleyCircumference = pulleyDiameter * 3.14159; // Pulley
circumference in cm
const float targetSpeed = 0.0167;    // Target speed in cm/s
const int motorSpeedRPM = (targetSpeed * 60) / pulleyCircumference; // RPM
calculation

// Stepper motor setup
Stepper stepper(stepsPerRevolution, 8, 10, 9, 11);

void setup() {
  stepper.setSpeed(motorSpeedRPM); // Set motor speed
  Serial.begin(9600);
  Serial.println("Stepper motor ready at 0.0167 cm/s.");
  Serial.print("Motor Speed (RPM): ");
  Serial.println(motorSpeedRPM);
}

void loop() {
  stepper.step(stepsPerRevolution); // Rotate one full revolution
  delay(60000); // Delay for 1 minute based on RPM
}
```

APPENDIX C: CAD designs

Figure C.1: Spring Designs

Figure C.2: Capsule Spring Configurations

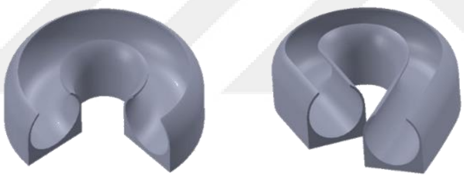

Figure C.3: 3. Intestine Models

CURRICULUM VITAE

Name Surname **:** Erfan PARSAEI

EDUCATION **:**

- **B.Sc.:** 2022, IAU of Tabriz, Faculty of Biomedical Engineering

PROFESSIONAL EXPERIENCE AND REWARDS:

- 2023 - 2025 EDL LAB Member at ISTANBUL Technical University